Mechanism for Major Disruptions in Tokamaks

B. V. Waddell,[a] B. Carreras,[b] H. R. Hicks, J. A. Holmes, and D. K. Lee
Oak Ridge National Laboratory, Oak Ridge, Tennessee 37830

(Received 1 May 1978)

We propose a mechanism for the major disruption in tokamaks that involves the nonlinear destabilization of tearing modes by the $(m=2)/(n=1)$ tearing mode, where m and n denote the poloidal and toroidal mode numbers, respectively. The magnetic islands generated can extend across the plasma cross section. For resistivities of the order of magnitude of these in TOSCA and LT-3, the time scale for their appearance is consistent with the time for the major disruption.

The magnitude of both the current and the density in present kokamak discharges is limited by the major disruptive instability,[1-5] which is characterized by a rapid (100 μsec) radial expansion of the plasma column. In this Letter, we consider a mechanism for the major disruption that involves the nonlinear interaction in three dimensions of tearing modes with different pitch. In cylindrical geometry, we find both analytically and numerically that the $(m=2)/(n=1)$ tearing mode (m and n are the poloidal and toroidal mode numbers, respectively) can nonlinearly destabilize other modes having odd m on a time scale consistent with the major distruptions if the 3/2 mode is also linearly unstable.

In order to study the nonlinear interaction of modes with different pitches, we employ the reduced set of equations derived in Refs. 6 in the large-aspect-ratio, low-β approximation. In terms of the poloidal flux function and the velocity stream function, the equations are

$$D\psi/Dt = \eta J_\zeta - E_\zeta{}^w - \partial\varphi/\partial\zeta, \tag{1}$$

$$DU/Dt = -S^2[\hat{\zeta}\cdot(\nabla\psi\times\nabla J_\zeta) + \partial J_\zeta/\partial\zeta]. \tag{2}$$

The radial, poloidal, and toroidal coordinates are denoted by r, θ, and ζ, respectively; η is the resistivity; and $E_\zeta{}^w$ is the electric field at the wall. The toroidal current density J_ζ is $\nabla_\perp{}^2\psi/\mu_0$, the velocity $\vec{V}_\perp$ is $\nabla\varphi\times\hat{\zeta}/B$, the vorticity U is $\nabla_\perp{}^2\varphi$, and $D/Dt \equiv \partial/\partial t + \vec{V}_\perp\cdot\nabla$; the subscript $\perp$ means perpendicular to the unit vector in the toroidal direction. The equations are in dimensionless form with all lengths normalized to radius a and all times normalized to the resistive magnetic diffusion time $\tau_R = \mu_0 a^2/\eta$ (where μ_0 is the vacuum magnetic permeability and η is the characteristic value of the resistivity). The quantity S is the ratio of τ_R and $\tau_{H,p} \equiv R_0(\mu_0\rho)^{1/2}/B_T$ (where R_0 is the major radius, ρ is the constant mass density, and B_T is the constant toroidal magnetic field). These equations have been numerically advanced in time employing a grid typically of size 60 (radial) by 30 (poloidal) by 15 (toroidal).

We consider safety-factor profiles of the form $q(r) = q(0)[1+(r/r_0)^{2\lambda}]^{1/\lambda}$, where $q(0)$ is the safety factor at $r=0$, r_0 is the width of the current channel, and λ is the flattening parameter. This profile is the same as the peaked, rounded, and flat profiles of Furth *et al.*[7] for $\lambda = 1$, 2, and 4, respectively. An analysis of this profile for $q(0)$ and $q(1)$ fixed at 1.08 and 4, respectively, shows that the 3/2 tearing mode, which is stable for $\lambda = 1$, becomes strongly unstable as λ increases; its (single-pitch) saturation width is also an increasing function of λ. Although the 2/1 mode is already unstable for $\lambda = 1$, its growth rate and saturation width also increase with λ. In addition, if $q(1)$ and λ are held fixed, then the growth rates and saturation widths of both the 2/1 and 3/2 modes increase with increasing $q(0)$.

On the basis of this analysis, we conclude that the most unstable profiles are the ones with large λ and $q(0)$ for which both the 2/1 and 3/2 modes have relatively large growth rates and saturation widths. The q profile corresponding to the electron temperature profile observed in the PLT tokamak before a disruption[3] can be described by this parametrization with $\lambda = 4$ and $q(0) = 1.38$ and $q(1) \sim 4$. The results we present here are mainly for this profile. This profile was also considered by White *et al.*[5]; however, only the 2/1 mode was studied because the two-dimensional code MASS was employed. We take $S = 1.3\times10^5$ (normalized at $r=0$), which corresponds to resistivities of the order of those in the TOSCA and LT-3 tokamaks. The resistivity is taken to be constant in time and given by $\eta(r) = E_\zeta{}^w/J_{\zeta 0}(r)$, where the subscript 0 denotes equilibrium quantities; of course, for large toroidal current deformations this model is not self-consistent. In a run, both the 2/1 and 3/2 modes are perturbed initially.

The basic results of the three-dimensional (3-D) calculations are summarized in Fig. 1, where the instantaneous growth rates of the 2/1 and 3/2 modes are plotted as functions of time (solid

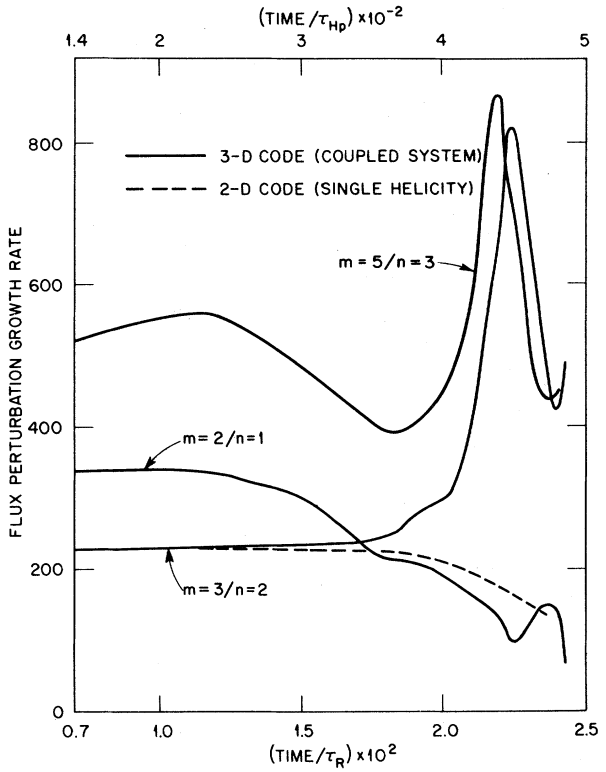

FIG. 1. The instantaneous growth rates of the 2/1 and 3/2 modes as a function of time; the solid and dashed lines are the numerical and model results, respectively.

lines). The growth rate of the 2/1 mode decreases in the same way that it does when only the 2/1 pitch is present. Although the growth rate of the 3/2 mode also decreases as the mode saturates if only that pitch is present, as indicated by the dotted line, in this three-dimensional run the 3/2-mode growth rate accelerates substantially and goes through a maximum or peak. Simultaneously, other modes are destabilized, particularly the 1/1 and 5/3 modes.

As the various modes are destabilized, the radial profile of the toroidal current density becomes much more severely deformed than in the two-dimensional case because islands of many different pitches develop as the growth rates peak. In Fig. 2, islands of various pitches are plotted near the end of the run. These flux contours were obtained by projecting from ψ modes of a given pitch and combining the projection with the 0/0 piece of ψ to define a helical flux function for that pitch. It is clear from Fig. 2 that overlapping islands develop, extending essentially from the plasma core to the limiter. Presumably, this island activity will lead to rapid transport of heat from the plasma center to the limiter because of the large parallel thermal conductivity.

Similarly numerical results have been obtained for other flat profiles for which the 2/1 and 3/2 modes are linearly unstable. We have studied several values of S and different initial conditions.

An analytic model has also been constructed. By evaluating the linear growth rates of the 3/2 and 5/3 modes including the 0/0 deformation of the equilibrium by the 2/1 mode (equivalent to a Δ' analysis of the perturbed equilibrium), one finds that although the growth rate of the 3/2 mode increases and the 5/3 mode becomes unstable, the magnitudes of the quasilinearly corrected growth rates are much smaller than those shown in Fig. 1. Consequently, a model that includes mode coupling as well as quasilinear theory must be constructed. Our analysis shows that the dominant effect that reduces the growth rate of the 2/1 mode is the quasilinear evoultion of the equilibrium (0/0 perturbation) caused by the 2/1 mode. The 1/1 and 5/3 modes are driven by the coupling of the 2/1 and 3/2 modes. The 3/2 mode is then in turn destabilized by coupling with the 1/1 and 5/3 modes through the 2/1 mode.

If we denote the Fourier components of ψ by ψ_{mn}, where m and n are the poloidal and toroidal mode numbers, respectively, and employ the WKB approximation

$$\psi_{mn}(t) \simeq \psi_{mn}{}^0 \exp[\int_{t_0}^{t} dt' \gamma_{mn}(t')],$$

where ψ_{mn} is the Fourier component at $t = t_0$, then a Fourier analysis of Eqs. (1) and (2) yields the following set of integral equations for the instantaneous growth rates:

$$\gamma_{11}(t) = \gamma_{53}(t) = \gamma_{21}(t) + \gamma_{32}(t), \quad (3)$$

$$\gamma_{21}(t) = \gamma_{21}{}^0 + g_1(\psi_{21}{}^0, \psi_{00}{}^0) \exp[\int_{t_0}^{t} dt' \gamma_{00}(t')], \quad (4)$$

$$\gamma_{00}(t) = 2\gamma_{21}{}^0 \exp\{\int_{t_0}^{t} dt' [2\gamma_{21}(t') - \gamma_{00}(t')]\}, \quad (5)$$

$$\gamma_{32}(t) = \gamma_{32}{}^0 + g_2((\psi_{21}{}^0, \psi_{11}{}^0) + (\psi_{21}{}^0, \psi_{53}{}^0), \psi_{32}{}^0) \times \exp\{\int_{t_0}^{t} dt' [2\gamma_{21}(t')]\}. \quad (6)$$

The quantities g_1 and g_2 are coupling coefficients that depend as indicated schematically on quantities at $t = t_0$, where t_0 is the time when linear eigenmodes have developed.

An analytic solution of Eqs. (3)–(6) can be constructed showing that a maximum occurs in the 3/2 growth rate provided $g_2 > 0$. This result can be obtained heuristically. Because the 3/2 mode is driven by the 2/1-1/1 and the 2/1-5/3 coupling,

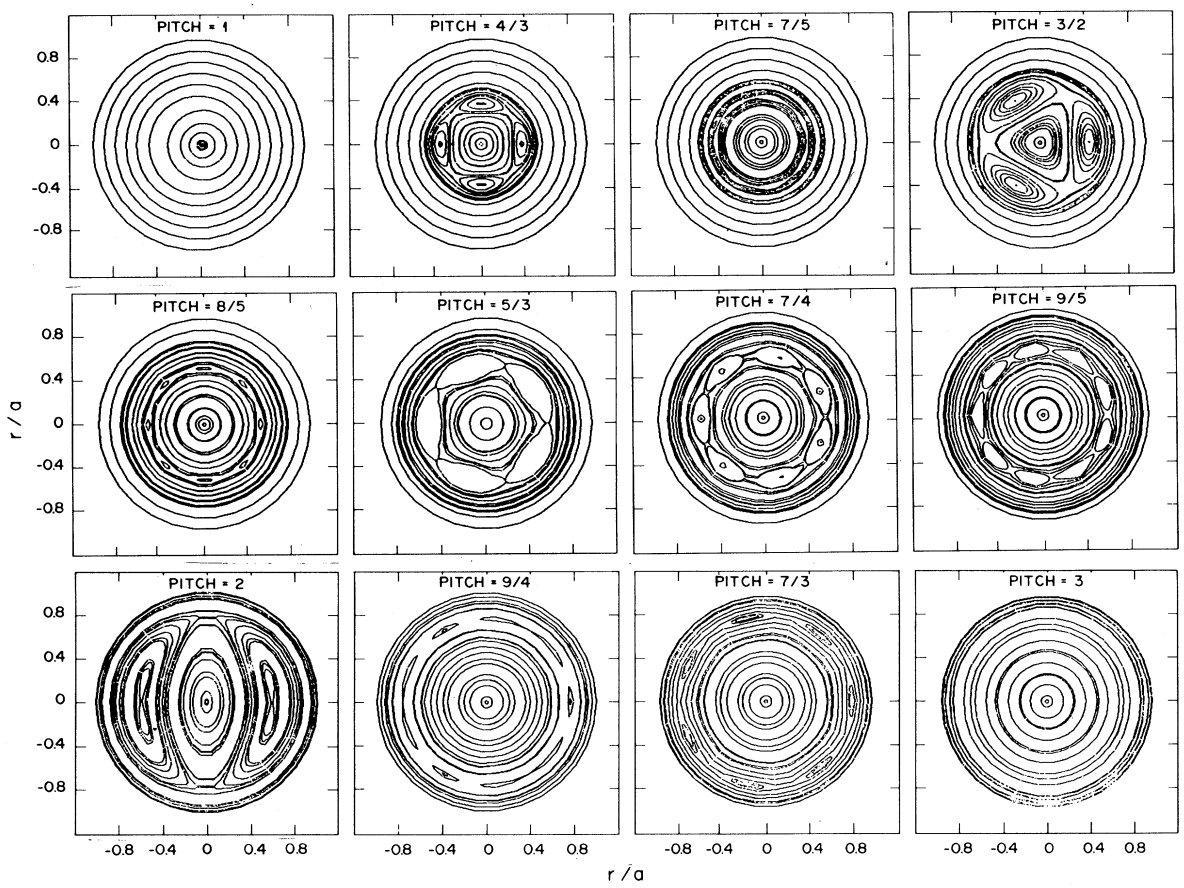

FIG. 2. Selected magnetic islands (obtained by projecting Fourier components of a given pitch) observed at time $t = 2.5\times10^{-1}\tau_R$.

its time rate of change is given by $d\psi_{32}/dt = \psi_{32}{}^0\psi_{32} + g_a\psi_{21}\psi_{11} + g_b\psi_{21}\psi_{53}$, where g_a and g_b are coupling coefficients. Then employing the WKB approximation, dividing by ψ_{32}, and noting from standard mode-coupling theory that Eq. (3) applies because the 1/1 and 5/3 modes are totally driven by the 2/1 and 3/2 modes, we obtain Eq. (6), where $g_2 = g_a\psi_{21}{}^0\psi_{11}{}^0/\psi_{32}{}^0 + g_b\psi_{21}{}^0\psi_{53}{}^0/\psi_{32}{}^0$. Clearly, if $g_2 > 0$, γ_{32} will increase initially. Because γ_{21} is decreasing, however, a maximum in γ_{32} should occur. Solution of Eqs. (3)–(6) shows that the position of the maximum is given by $\Delta t \equiv t^M - t_0 = [\ln(2\gamma_{21}{}^0/|g_1|)]/2\gamma_{21}{}^0$ and the value is given by $\Delta\gamma \equiv \gamma_{32}{}^M - \gamma_{32}{}^0 = g_2\gamma_{21}{}^0/2|g_1|$, where the superscript M denotes quantities at the peak. Because of the way in which the coupling coefficients scale with the parameters at $t = t_0$, Δt and $\Delta\gamma$ scale in the following fashion for a particular q profile: $(\Delta t)' = (\gamma_{21}{}^0\Delta t - \ln\epsilon)/(\gamma_{21}{}^0)'$ and $(\Delta\gamma)' = (\gamma_{32}{}^0)'\Delta\gamma/\gamma_{32}{}^0$, where ϵ denotes the magnitude of ψ_{21}', the unprimed variables indicate quantities determined from an arbitrary run, and the primed variables are quantities for another run with a similar q profile but a different value of S. Rather than compute g_1 and g_2 analytically, which is a difficult task because of the many tearing layers involved, we determined them by using the preceding expressions for Δt and $\Delta\gamma$ to fit the data for one run; then we use the scaling rules for other runs and for large S values that cannot be analyzed with the code because of the small tearing layer widths involved. But we have preliminary results from a more efficient code which show the same characteristics for $S = 10^6$ at $r = 0$. The fit for the run described in the preceding paragraphs is shown in Fig. 1 (dashed lines). An analysis of several runs verifies the scaling rules for Δt and $\Delta\gamma$.

The mechanism described here is generally consistent with the experimental data on the major disruption obtained in the LT-3 and PLT devices. For example, in LT-3, the toroidal probes show the presence of $n = 1$ and $n = 2$ modes, the poloidal probes show the presence of $m = 1$, 2,

and 3 modes, and the combination $m = 3$ and $n = 2$ has been detected.[2] In addition, in PLT[3] although $m = 2$ precursor oscillations are observed, the disruption itself often exhibits poloidal asymmetry, presumably corresponding to the generation of odd poloidal mode numbers. Finally, during the disruption $m = 1$ oscillations are often observed within the plasma core; this observation might correspond to the generation of the $m = 1$ mode described here.

The most important feature of the major disruption that any model must explain is the rapid time scale. For the mechanism described here, the characteristic time scale for the development of the magnetic islands is the width of the peak in the 3/2 growth rate. If we define the half-width Γ by $\gamma_{32}(t^M \pm \Gamma) - \gamma_{32} = \Delta\gamma/2$, then $\Gamma \simeq (\gamma_{21}{}^0)^{-1}$. Assuming that the scaling does hold for all values of S, we find that in PLT the predicted value for the disruption time is 230 μsec. If the effect of diamagnetic drifts is included in the expression for $\gamma_{21}{}^0$, then $\Gamma \simeq 440$ μsec. These time scales are consistent with the observed disruption time of 500 μsec. A study of several other machines, including LT-3 and TOSCA for which the preceding analysis rigorously applies as far as the magnitude of the resistivity is concerned, also shows consistency with the observed disruption time (approximately 10 μsec).

This research was sponsored by the Office of Fusion Energy, U. S. Department of Energy, under Contract No. W-7405-eng-26 with the Union Carbide Corporation.

[a]Deceased.

[b]Visitor from Junta de la Energía Nuclear, Madrid, Spain.

[1]E. P. Gorbunov *et al.*, Sov. At. Energ. 15, 1105 (1963); L. A. Artsimovich *et al.*, in *Proceedings of the Fifth International Conference on Plasma Physics and Controlled Nuclear Fusion Research, Tokyo, Japan, 1974* (International Atomic Energy Agency, Vienna, Austria, 1975); F. Karger *et al.*, in *Proceedings of the Sixth International Conference on Plasma Physics and Controlled Nuclear Fusion Research, Berchtesgaden, West Germany, 1976* (International Atomic Energy Agency, Vienna, 1977), Vol. 1, p. 267; Equipe TFR, *ibid.*, p. 279; S. V. Mirnov *et al.*, *ibid.*, p. 291.

[2]I. Hutchinson, Phys. Rev. Lett. 37, 388 (1976); D. B. Albert *et al.*, Nucl. Fusion 17, 863 (1977); D. B. Albert (The Australian National University), private communication.

[3]N. R. Sauthoff *et al.*, Princeton Plasma Physics Laboratory Report No. PPPL-1379, 1978 (unpublished).

[4]M. N. Rosenbluth *et al.*, Phys. Fluids 16, 1894 (1973); M. N. Rosenbluth *et al.*, Phys. Fluids 19, 1987 (1976); R. Y. Dagazian, Nucl. Fusion 16, 123 (1976); B. Kadomtsev, in *Proceedings of the Sixth International Conference on Plasma Physics and Controlled Nuclear Fusion Research, Berchtesgaden, West Germany, 1976* (International Atomic Energy Agency, Vienna, 1977), Vol. 1, p. 555; J. M. Finn, Phys. Fluids 20, 1749 (1977).

[5a]R. B. White *et al.*, in *Proceedings of the Sixth International Conference on Plasma Physics and Controlled Nuclear Fusion Research, Berchtesgaden, West Germany, 1976* (International Atomic Energy Agency, Vienna, 1977), Vol. 1, p. 569; D. Biskamp *et al.*, *ibid.*, p. 579.

[5b]R. B. White *et al.*, to be published.

[5c]R. B. White *et al.*, Phys. Rev. Lett. 39, 1618 (1977).

[6]H. R. Strauss, Phys. Fluids 19, 134 (1976); H. R. Hicks *et al.*, ORNL Report No. ORNL/TM-6096, 1977 (unpublished); D. Biskamp (Max-Planck Institut), private communication.

[7]H. P. Furth *et al.*, Phys. Fluids 16, 1054 (1973).

Superfluid Solitons in Helium Films

B. A. Huberman
Xerox Palo Alto Research Center, Palo Alto, California 94304

(Received 10 July 1978)

It is shown that in monolayer superfluid He^4 films, in addition to third-sound modes, small amplitude effects can lead to the existence of gapless solitons made up of superfluid condensate. These nonlinear excitations can be created by localized perturbations in the superfluid density. The conditions are studied under which such initial disturbance evolves into an ordered string of solitons, and the differences to be expected in thicker films are discussed.

Third-sound phenomena in helium films have provided a wealth of information on the properties of nearly two-dimensional superfluids.[1] Originally proposed by Atkins[2] as the superfluid analog of surface waves, they soon became a precise tool for examining the critical behavior of

